JOC The Journal of Organic Chemistry

Article

pubs.acs.org/joc

Electron-Rich Triphenylamine-Based Sensors for Picric Acid Detection

Aniket Chowdhury and Partha Sarathi Mukherjee*

Department of Inorganic and Physical Chemistry, Indian Institute of Science, Bangalore 560 012, India

Supporting Information

ABSTRACT: This paper demonstrates the role of solvent in selectivity and sensitivity of a series of electron-rich compounds for the detection of trace amounts of picric acid. Two new electron-rich fluorescent esters (**6**, **7**) containing a triphenylamine backbone as well as their analogous carboxylic acids (**8**, **9**) have been synthesized and characterized. Fluorescent triphenylamine coupled with an ethynyl moiety constitutes π-electron-rich selective and sensitive probes for electron-deficient picric acid (PA). In solution, the high sensitivity of all the sensors toward PA can be attributed to a combined effect of the ground-state charge-transfer complex formation and resonance energy transfer between the sensor and analyte. The acids **8** and **9** also showed enhanced sensitivity for nitroaromatics in the solid state, and their enhanced sensitivity could be attributed to exciton migration due to close proximity of the neighboring acid molecules, as evident from the X-ray diffraction study. The compounds were found to be quite sensitive for the detection of trace amount of nitroaromatics in solution, solid, and contact mode.

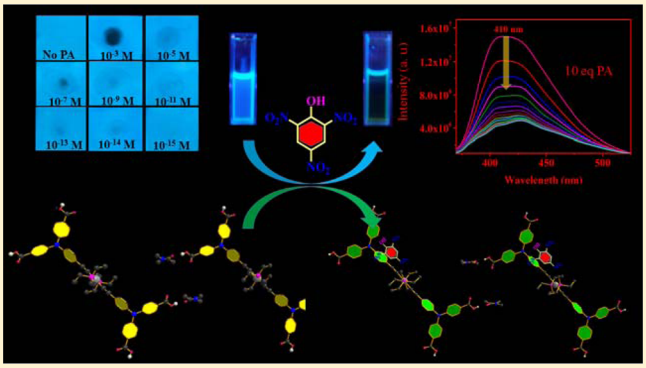

INTRODUCTION

Well-organized terror attacks around the world in recent times have prompted researchers to find effective ways to detect explosives. Many common explosives contain nitro compounds as primary constituents. TNT was the most popular choice among NACs until World War I.[1−4] However, picric acid (PA) has also emerged as a potential substitute due to its high explosive power. In addition, because it is highly water soluble, PA is a major contaminate of groundwater. It is widely used in the dye industry, rocket fuel manufacturing, and the pharmaceutical industry.[5,6] Intake of PA causes skin and eye irritation, liver malfunction, and chronic diseases like anemia, cancer, and cyanosis.[7−9] Thus, for social and environmental safety, effective monitoring and detection of trace amounts of PA, both in solution and vapor phase, is quite important.[10,11]

Different techniques (spectroscopic, electrochemical)[12,13] and materials (small molecule sensors,[14] nanoparticles,[15] nanofibers,[16] polymers,[17] gels,[18] MOFs,[19] etc.) have been used for PA detection in solution and the vapor phase. Among them, fluorescence signaling is a potential choice because of its high sensitivity, quick response, cost efficiency, portability, and easy sample preparation. In the past few years, different types of effective fluorescent sensors emerged for PA. Although the first selective sensor for PA was reported in 2004, this field needs to be explored further for suitable sensors.[20] In 2011, intermolecular charge transfer (ICT) based probes were reported by our group and Kumar et al.[14,21] Very recently, the first fluorescence nonquenching ratiometric probe was also reported.[22] However, many of the previous reported sensors had several drawbacks which include low binding affinity to PA and interference from other nitro compounds, but most importantly, they were deprived of sensitivity toward PA vapor which can be attributed due to lack of signal amplification effect.

The signal amplification effect was first reported in 1998 for detection of trace amounts of explosives in the vapor phase by conjugated polymers through exciton migration.[23] Conventional conjugated polymers owing to their very high molecular weight have poor solubility in common organic solvents, which reduces their sensitivity and reusability with number of use. Therefore, an alternative approach is required to design a system which can easily be fabricated and also facilitates exciton migration. Supramolecular polymer turns out to be a potential candidate in this regard. In a supramolecular polymer, multiple molecules self-organize by noncovalent interactions like H-bonding, van der Waals, $\pi-\pi$ interactions, etc. to form an infinite network having a well-defined motif.[24] Recently, our group reported a series of supramolecular polymers for nitroaromatics detection where carboxylic acid with anthracene and pyrene backbones were used for detection of trace amount of explosives in vapor phase.[25] The carboxylic acid group is known to form a dimer structure by intermolecular H-bonding.[26] From single-crystal X-ray and scanning tunneling

Received: February 18, 2015
Published: March 30, 2015

ACS Publications © 2015 American Chemical Society

DOI: 10.1021/acs.joc.5b00348
J. Org. Chem. 2015, 80, 4064−4075

Scheme 1. Synthesis of Compound 5

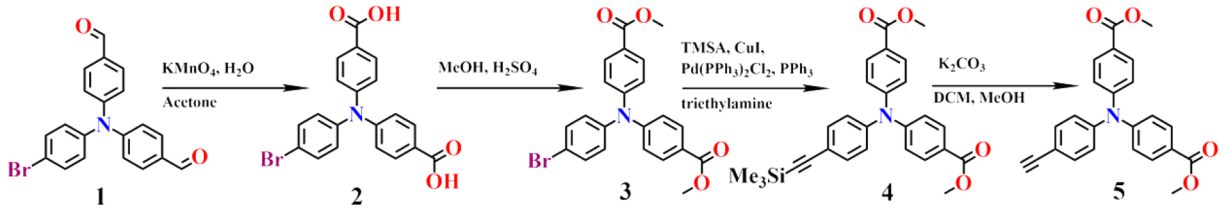

Scheme 2. Synthesis of Compounds 6–9

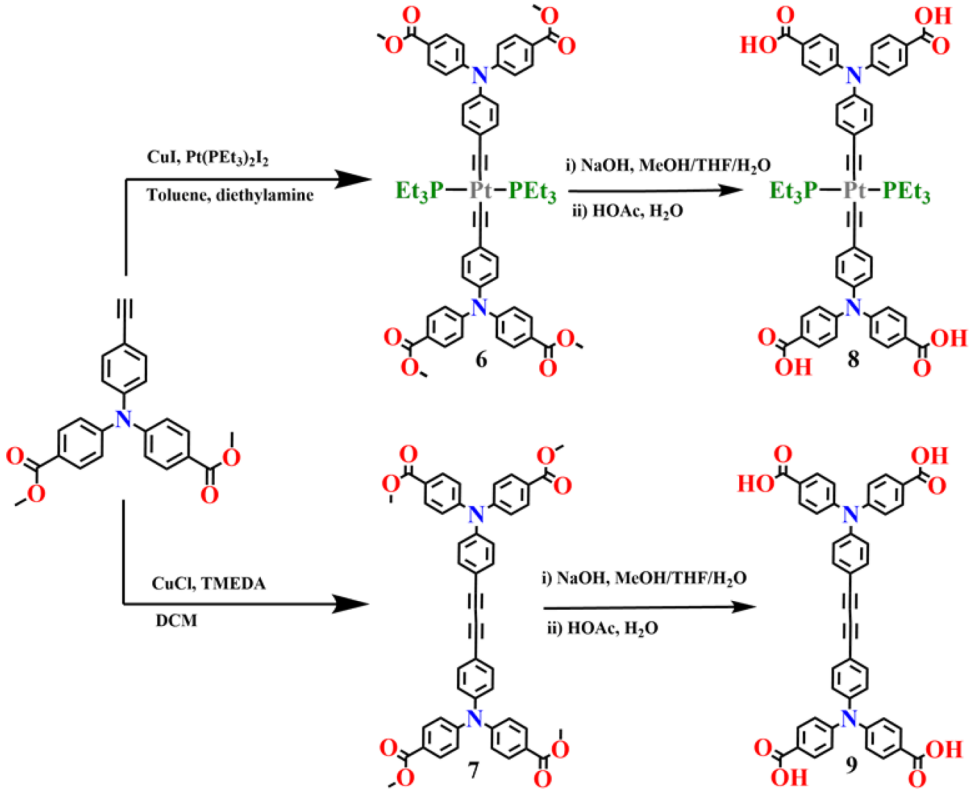

microscopy (STM) analysis, signal amplification mechanism in the solid state is already well established in the literature.[25] During solution-state quenching only the sensor–solvent interaction was explored, leaving out the analyte–solvent interaction. The solvent molecules interact with the sensor and analyte with different types of interactions including H-bonding and acid–base, which along with stabilization could alter their photophysical properties. Therefore, to explore the role of solvent molecules in solution-state sensing of nitroaromatics and to propose a proper mechanism through which the quenching takes place, we report here the synthesis and photophysical properties of four compounds comprised of triphenylamine backbone. The synthesis of the compounds **6–9** is shown in Schemes 1 and 2.

RESULT AND DISCUSSION

Synthesis and Characterization of the Compounds 6–9. For constructing the desired sensors, we chose triphenylamine (TPA) as the fluorophore. TPA as fluorophore has found application in solid-state emitters,[27] biomarkers,[28] aggregation induced emissive (AIE) materials, etc.[29] To the best of our knowledge, only a few reports are known on TPA-based PA sensors.[30] Conjugated polyaromatic systems are prone to form aggregates in solution by $\pi-\pi$ interaction, decreasing fluorescence intensity by aggregation-caused quenching (ACQ).[31] Thus, to block aggregate formation we have also incorporated the bulky $Pt(PEt_3)_2$ moiety at the center of the sensors. We assumed that bulky $-Pt(PEt_3)_2$ might not only restrict closely packed aggregate formation in solution, but in the solid state it might make the system more porous; thus, nitroaromatic vapors could diffuse through the medium for better response. To verify the effect of bulky substituent on sensing, another set of analogous sensors without the $Pt(PEt_3)_2$ was designed as model compounds. Therefore, two ethynyl-functionalized TPA compounds were designed and synthesized for selective and sensitive detection of PA as shown in Schemes 1 and 2.

Compounds **6–9** were characterized by ^1H NMR, ^{13}C NMR, ^{31}P NMR, IR, and HRMS (Supporting Information). The molecular structures of **7** and **8** were confirmed by single-crystal X-ray diffraction studies (Figures 1 and 2 and Table 1). Single crystals of **7** were obtained by slow evaporation of $CHCl_3$ solution. The compound crystallized in the monoclinic system with the $P2_1/n$ space group. Solid-state structural analysis of **7** (Figure 1) revealed that each neighboring molecule was oriented in a zigzag manner prohibiting direct or through-

DOI: 10.1021/acs.joc.5b00348
J. Org. Chem. 2015, 80, 4064–4075

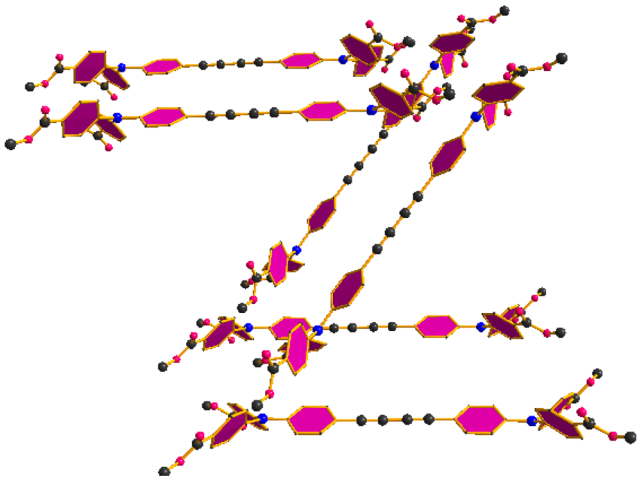

Figure 1. Crystal structure of 7 (color codes: red = O, black = C, blue = N).

space interaction, while the methyl groups hindered close packing of the compound. Single crystals of **8** were obtained by slow evaporation of saturated $CHCl_3$−dimethylacetamide (DMA) solution of the compound. It was crystallized in a triclinic system with $P\bar{1}$ space group. Careful inspection revealed that each molecule was surrounded by four DMA molecules which were H-bonded to the terminal −COOH groups, but the neighboring molecules were oriented in a regular repetitive pattern which was important for through-space exciton migration (Figure 2).

Photophysical Properties. Compounds **6** and **7** were highly soluble in chloroform/dichloromethane, while **8** and **9** were soluble in DMA, dimethylformamide (DMF), and dimethyl sulfoxide (DMSO) (Table 2). Thus, photophysical studies were performed in $CHCl_3$ (**6** and **7**) and DMA (**8** and **9**). Compounds **6** and **8** showed single absorption peaks at 358 nm, corresponding to the $\pi-\pi^*$ transition of the conjugated TPA core, and compounds **7** and **9** exhibited broad absorption peaks with multiple absorption maxima spanning from 350 to 390 nm (Figure 2).[32] Upon excitation at absorption maxima, they exhibited emission with maxima ranging from 420 to 460 nm (Figure 3).

Aggregate Formation of the Compounds. It is well documented in the literature that planar polyaromatic compounds in solution form aggregates through $\pi-\pi$ interaction.[33] Thus, the aggregate formation of these compounds was investigated by particle size measurement. The self-association behavior could also be explored by concentration-dependent UV−vis spectroscopic analysis, but at higher concentration the absorbance of the compounds exceeded the instrument limit. Thus, we focused on the concentration-dependent fluorescence and particle size determination of the compounds to explore the self-association behavior.

Table 1. Crystallographic Data and Refinement Parameters for Compounds 7 and 8

compd	7	8
emp formula	$C_{48}H_{36}N_2O_8$	$C_{56}H_{58}N_2O_8P_2Pt$
Fw	768.79	1143.3316
T (K)	298	298
crystal system	monoclinic	triclinic
space group	$P2_1/n$	$P\bar{1}$
a (Å)	11.69(18)	7.707(5)
b (Å)	10.22(16)	9.741(5)
c (Å)	16.90(3)	27.780(5)
α (deg)	90	94.515(5)
β (deg)	96.57(4)	96.731(5)
γ (deg)	90	93.585(5)
V (Å^3)	2007.5	2059.32
Z	2	1
ρ_{calc} (g cm^{-3})	1.272	1.203
μ(Mo Kα) (mm^{-1})	0.087	0.087
λ (Å)	0.71073	0.71073
F(000)	804.4	1051
no. of collected reflns	39786	7250
no. of unique reflns	3534	6895
goodness of fit (F^2)	1.060	0.784
R_1 $[I > 2\sigma(I)]^a$	0.0483	0.0615
$wR_2[I > 2\sigma(I)]^b$	0.1419	0.1618

$^aR_1 = \Sigma||F_o| - |F_c||/\Sigma|F_o|$. $^bwR_2 = (\Sigma[w(F_o^2 - F_c^2]/\Sigma[w(F_o^2)^2)^{1/2}$.

Table 2. Spectroscopic Properties of 6−9 in $CHCl_3$ and in DMA

compd	Abs λ_{max} (nm)	ε (M^{-1} cm^{-1})	Ems λ_{max} (nm)	ϕ	τ (ns)
8	356	78790	450	0.12	0.43
6	355	137670	414	0.23	0.50
9	350, 370, 395	93510	427	0.19	0.28
7	353, 374, 395	165950	416	0.34	0.34

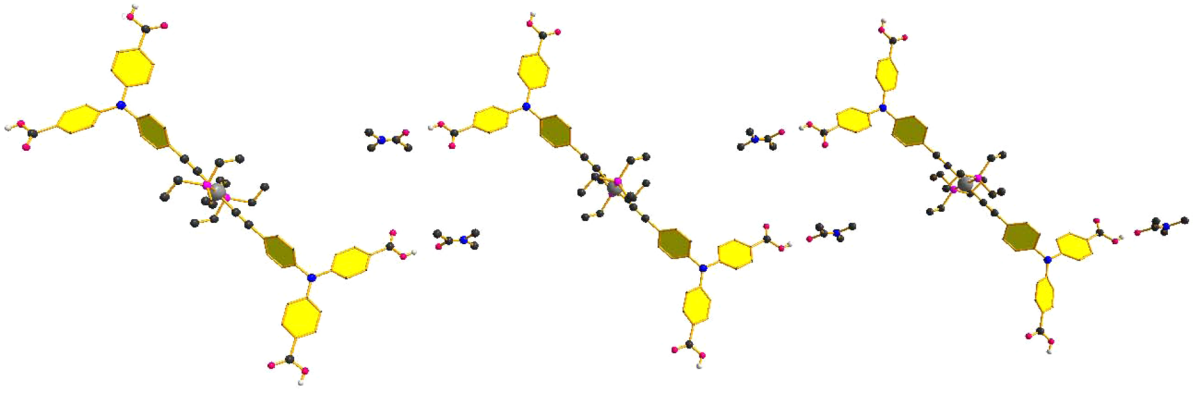

Figure 2. Single crystal structure of **8** (color codes: red = O, black = C, blue = N, gray = Pt, pink = P, white = H).

DOI: 10.1021/acs.joc.5b00348
J. Org. Chem. 2015, 80, 4064−4075

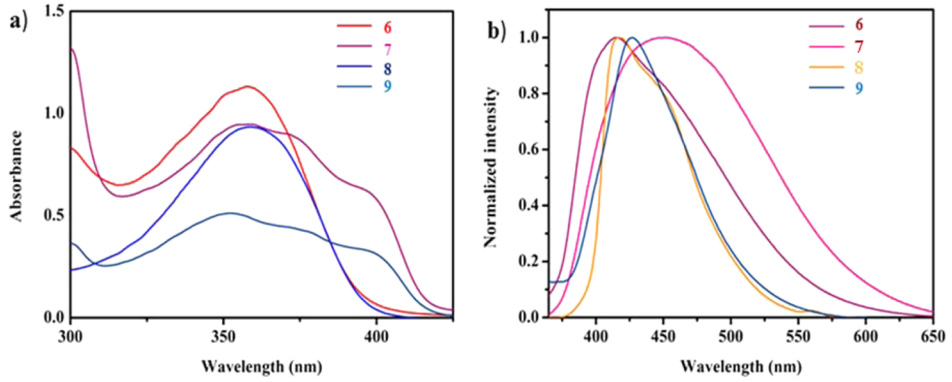

Figure 3. (a) Absorption spectra of the compounds in $CHCl_3$ and DMA. (b) Normalized emission spectra of the sensors in $CHCl_3$ and DMA.

Concentration-Dependent Fluorescence. The concentration-dependent fluorescence spectra of **8** in DMA is represented in Figure 4. At higher concentration (10^{-3} M), a

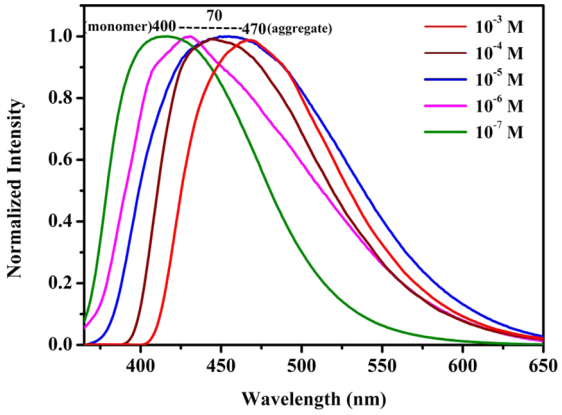

Figure 4. Concentration-dependent fluorescence of **8** in DMA.

broad peak was observed at 470 nm, and upon dilution this peak vanished and a new peak appeared at 420 nm. The broad band at 470 nm was attributed to the self-assembled aggregates in the solution. Upon dilution the aggregates dissociated to form a monomer that exhibited emission at 420 nm. The other sensors also revealed similar concentration-dependent fluorescence change in corresponding solutions (Supporting Information).

Particle Size Measurement of the Compounds. The particle size was measured by the dynamic light scattering (DLS) method. Solutions of **6** and **8** in different concentration ranging from 10^{-3} to 10^{-5} M were considered for the DLS experiment, and different particle sizes were found (Figure 5). The average aggregate size of **8** in highly concentrated sample was around 701 nm, and the very broad distribution indicated the presence of various sizes of aggregates in the medium. When diluted, the distribution was narrow and the aggregate size also decreased to ~310 nm in 10^{-4} M solution. However, for **6** the similar concentrated solutions exhibited lower particle size. The most concentrated solution (10^{-3} M) had a particle size of about 389 nm, which was comparatively much lower than 701 nm, and the other two solutions had particles ranging from 209 to 150 nm. This variation in size was attributed to deviation in the number of molecules available for $\pi-\pi$ stacking in solution. Compounds **7** and **9** revealed a similar trend of concentration-dependent variation of particle size.

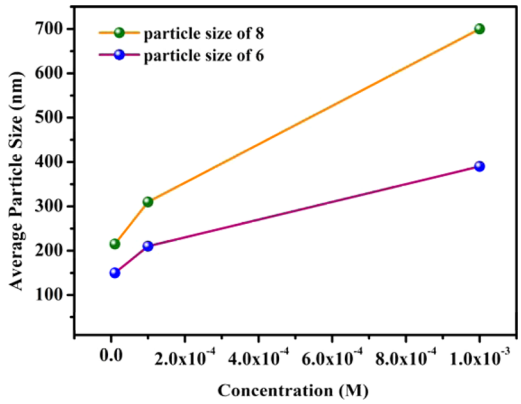

Figure 5. Particle size variation of **8** in DMA and **6** in $CHCl_3$ upon changing the concentration from 10^{-3} to 10^{-5} M.

UV–vis Titration Experiments. The sensors displayed rapid change in photophysical properties with varying concentration as evident from DLS experiments and concentration-dependent fluorescence study. For practical purposes, the sensor must be uniform throughout the medium. For UV–vis titration dilute solutions of the compounds (10^{-5} M) were titrated with PA (10^{-3} M), and the corresponding responses are shown in Figure 6. When compound **8** was titrated with PA as analyte a new intense band at a higher wavelength was observed. Moreover, the color of the compound immediately changed from colorless to intense yellow probably due to the formation of either charge-transfer complex or picrate anion. This new low energy band was proposed to be the charge-transfer band. Titration with **9** also showed similar charge transfer band, but for **6** and **7** the bands were very weak (Supporting Information).

Fluorescence Titration of Nitroaromatics. At concentrations higher than 10^{-7} M, the compounds existed in aggregate–monomer equilibrium; thus, the homogeneity of the system was disrupted. As the molecules in aggregate form could not participate in analyte quenching, the presence of aggregate would reduce the efficiency of the sensors. Thus, for the fluorescence titration experiment a small amount of PA (10^{-5} M) was gradually added to a dilute solution (10^{-7} M) of the sensors. The emission intensity of **8** steadily quenched upon addition of small amount of PA, and no residual emission was observed, whereas for **6** emission intensity was almost retained even after addition of excess PA (Figure 7). Thus, **6** and **8** showed considerable difference in their quenching efficiency

DOI: 10.1021/acs.joc.5b00348
J. Org. Chem. 2015, 80, 4064–4075

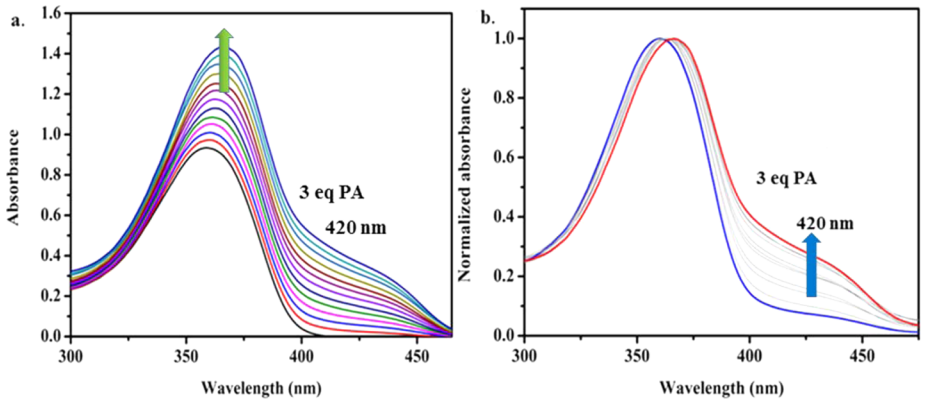

Figure 6. (Left) UV/vis spectra of PA titration with **8** in DMA. (Right) Normalized spectra.

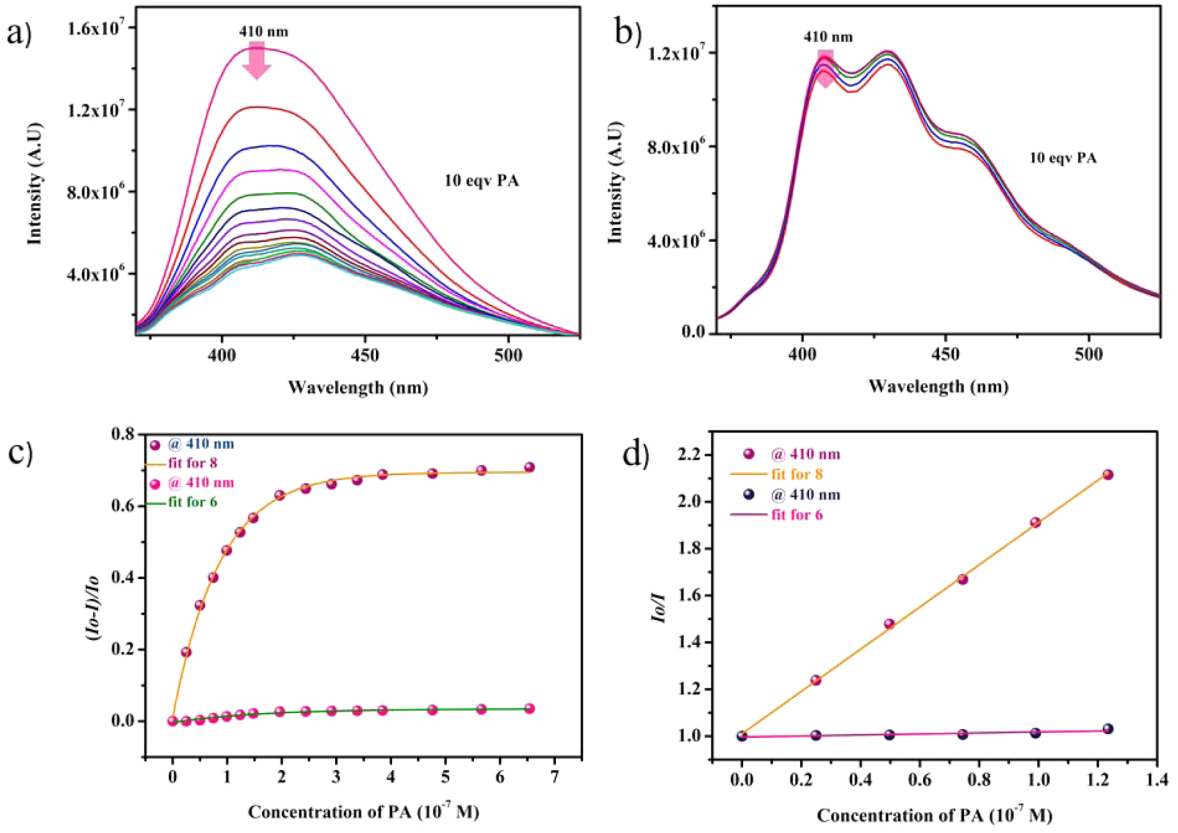

Figure 7. Titration with PA: (a) **8** in DMA and (b) **6** in $CHCl_3$. (c) Quenching efficiency plot of **6** and **8**. (d) Stern–Volmer plots of **6** and **8**.

and quenching rate. To gain a better understanding of quenching rate the Stern–Volmer constant was calculated.

The Stern–Volmer equation is expressed as

$$I_0/I = 1 + K_{SV}[Q]$$

where I_0 and I are the initial and final fluorescence intensities after addition of analyte and [Q] is the analyte concentration. This simple equation turns complex when more than one type of quenching mechanisms work simultaneously. Two types of quenching mechanisms are common, static and dynamic, and they often work together.

The existence of static quenching by a ground-state charge-transfer complex was verified from UV–vis titration of the compounds with picric acid.

The existence of dynamic quenching could be elucidated from the fluorescence lifetime measurement of the sensors with the addition of different amounts of analyte. To find out whether dynamic quenching was occurring we checked the analyte concentration dependent fluorescence lifetime for the compounds **8** and **9** and found no change in excited-state lifetime, which implied the occurrence of static quenching only (Supporting Information).[34]

Compounds **8** and **9** have very high quenching efficiency toward PA as is evident from their Stern–Volmer constants (5.72×10^6 M^{-1} for **8** and 2.9×10^5 $M^{-1}$for **9**). As mentioned previously, the acids **8** and **9** showed higher affinity for PA compared to the ester analogues (Supporting Information). This very high sensitivity was further investigated by NMR titration experiment. The detection limit for **8** and **9** was calculated to be ~5 ppb following the previously reported procedure in literature.[35,36]

DOI: 10.1021/acs.joc.5b00348
J. Org. Chem. 2015, 80, 4064–4075

Response toward Other NAC's. Along with PA, several other nitro compounds like trinitrotoluene (TNT), 2,4-dinitrophenol (2,4-DNP), 2,4-dinitrotoluene (DNT), 3,4-DNT, 1,3-dinitrobenzene (DNB), 4-nitrobenzoic acid (DBA), nitrotoluene (3-NBA), nitrobenzene (NB), and nitromethane were used to check the selectivity of the sensors (Figure 8).

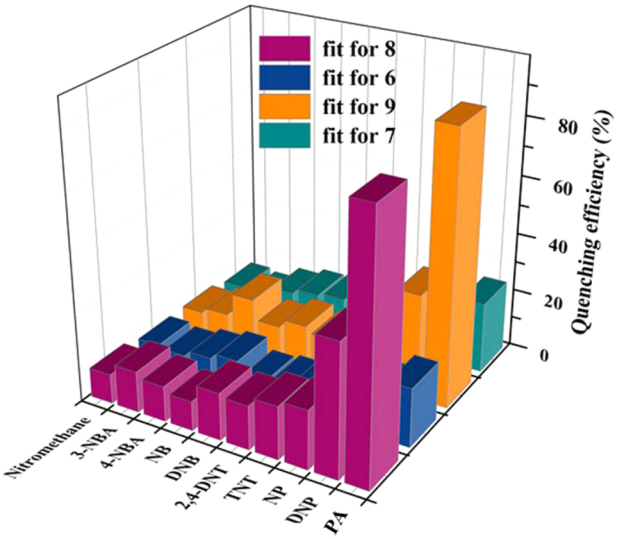

Figure 8. Quenching efficiency of **6** and **7** in $CHCl_3$ and **8** and **9** in DMA with different nitro compounds.

Except 2,4-DNP, all other compounds showed insignificant quenching of the emission intensity. The quenching efficiency of DNP was less than 40% for both the acids, but monosubstituted nitrophenols did not exhibit any considerable quenching behavior.

NMR Titration Experiment. To explore the mechanism and to identify the actual binding position of PA, ^{1}H NMR titration was performed with **8** in DMSO-d_6 (Figure 9). We observed that with the addition of PA all the protons shifted to a more shielded region. If PA withdraws electron density from the compound it should show a downfield shift. It is only possible if electron density was transferred from PA to the sensor. From the spectral shift it was observed that the aromatic protons near the ethynyl moiety underwent the maximum chemical shift, whereas the protons attached to terminal phenyl rings had a negligible chemical shift. The significant change in the chemical shift of protons near the ethynyl group suggested that the benzene ring near the ethynyl group acts as the receptor site.

When the NMR spectra of **7** and **9** were compared we found that the aromatic peak corresponding to PA was at 8.63 in DMSO-d_6 and at 9.3 in $CDCl_3$ (Supporting Information). When compared with previous reports, we found that the chemical shift of the aromatic proton of picrate was also 8.62 in DMSO-d_6.[14,37] Thus, we assume that solvents like DMA, DMSO, and even water present in the medium could interact with PA. PA being highly acidic in nature has a tendency to form picrate in DMA/DMSO to be stabilized by ion-pair interaction. This highly electron-rich picrate molecule could donate electrons to the sensors, which was established from the upfield shift of the aromatic protons of the sensor (Supporting Information). Previously, we studied the photophysical properties of **6** and **7** in $CHCl_3$. As evident from our observation, PA cannot form picrate in $CHCl_3$. Therefore, to explore the interaction of picrate with **6** and **7** we prepared picrate solution in $CHCl_3$ by adding an equivalent amount of triethylamine (NEt_3) in the medium. Compound **7** showed a significant change in UV–vis and fluorescence upon gradual addition of picrate to the medium (Figure 10).

Compound **6** also exhibited similar photophysical changes. Thus, the ester analogues **6** and **7** were also highly sensitive toward picrate, and depending on the solvent used, they exhibited different sensitivity toward PA. When picrate was

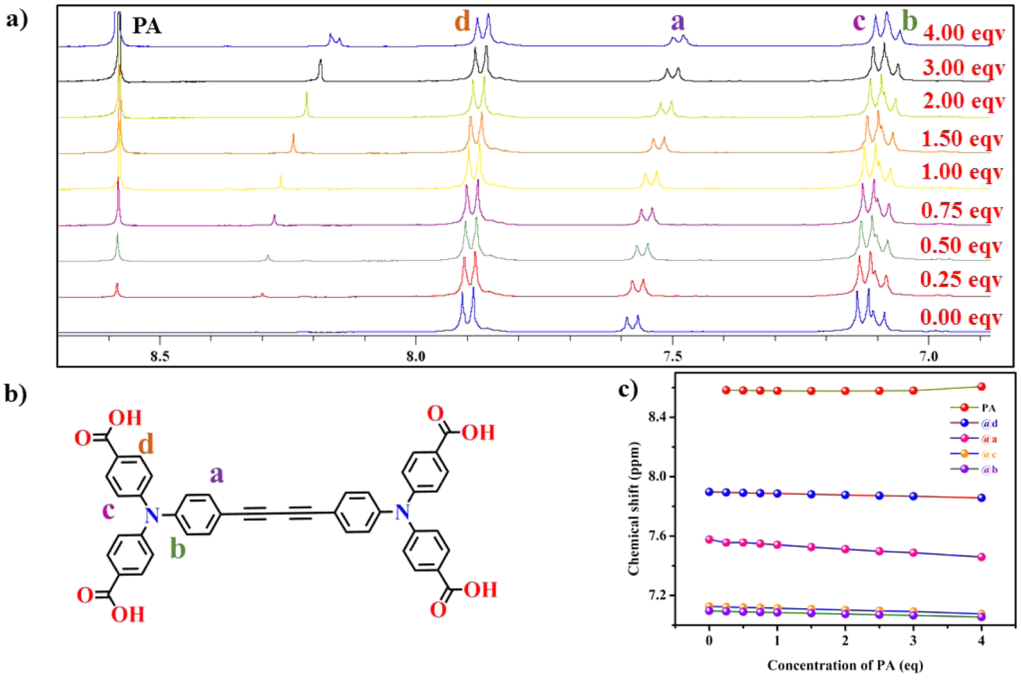

Figure 9. (a) Chemical shift change during NMR titrations, (b) peak positions of the protons in compound **9**, and (c) chemical shift change of the protons with change in concentration of PA.

DOI: 10.1021/acs.joc.5b00348
J. Org. Chem. 2015, 80, 4064–4075

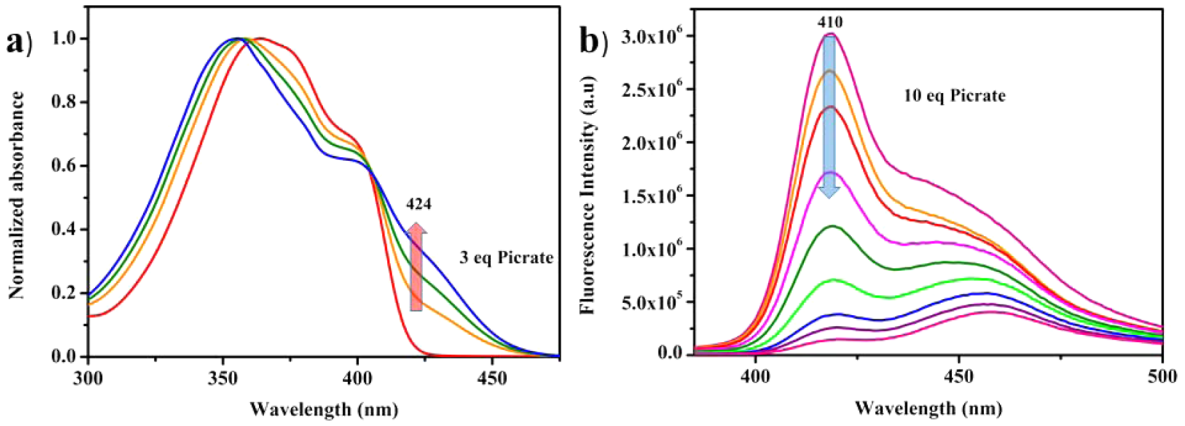

Figure 10. (a) UV−vis titration of **7** with picrate in $CHCl_3$ and (b) fluorescence titration in $CHCl_3$.

chosen as analyte all of the compounds showed similar changes in their photophysical response. Thus, the compounds **8** and **9** did not have any superior sensitivity to PA than **6** and **7** in solution.

Solution-Mode Detection. Along with change in fluorescence signaling, many sensors are reported to show visual color change upon PA addition to the sensor solution.[14] Thus, solution-mode visual detection of PA is important for real time application. Thus, for visual detection, 10^{-5} M PA was slowly added to 10^{-7} M solutions of **8** in incremental fashion as shown in Figure 11. Upon PA addition the fluorescence quenched from blue to nonfluorescent, which was consistent with the previously obtained result.

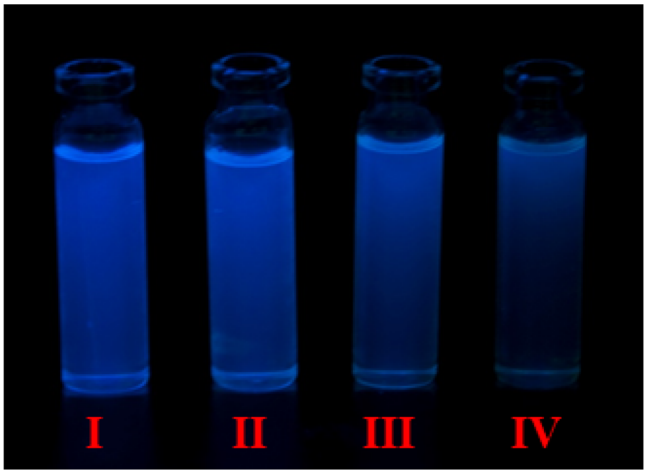

Figure 11. Visual color change under UV light upon gradual addition of 10^{-5} M PA in $CHCl_3$ to 4 mL of 10^{-7} M solution of **8** in DMA, (**I**, 0 μL of PA; **II**, 20 μL of PA; **III**, 40 μL of PA; **IV**, 80 μL of PA).

Contact-Mode Detection. We have performed the fluorescence titration experiment of the sensors with PA in highly dilute solution 10^{-7} M. Considering the factors of portability and cost-efficiency, we prepared test strips from commercially available Whatman filter paper. For contact-mode sensing, Whatman 42 filter paper was cut into 2 cm^2 pieces and dipped into the concentrated solution of **8** for 10 min and subsequently dried under reduced pressure for 2 h. For the experiment, PA solutions of different concentrations were prepared (10^{-3}−10^{-15} M), and 10 μL of each solution was drop-casted on each fresh test strip (Figure 12). When the strips were monitored under UV light, dark black spots were observed for PA. The spots were prominent for concentrated sample and slowly faded upon dilution.

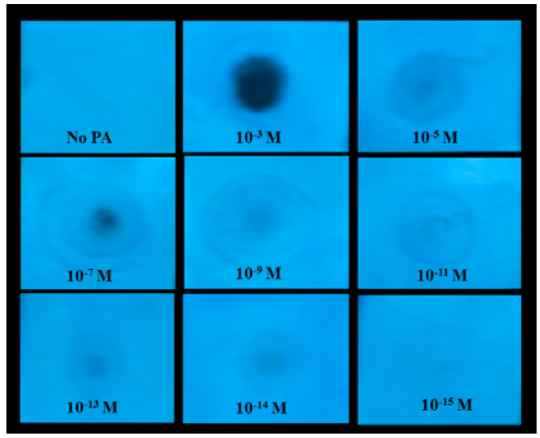

Figure 12. Paper strip images of the sensor **8** after addition of different concentrations of PA.

Solid-State Sensing. As mentioned in the Introduction, our prmary aim was to investigate the solution-state quenching mechanism of sensor with PA; therefore, we designed and explored the change in solution-state photophysical preoperties of the sensors in the presence of different NACs. We were also interested to investigate if the compounds were potential for solid-tate sensing. For solid-state experiments, different nitroaromatics were used. Nitrobenzene (NB) has the highest vapor pressure among the used nitroaromatics in the present paper; therefore, we initially exposed the compound in NB vapor (Figure 13). The initial fluorescence intensity of all of the compounds decreased upon exposure to NB vapor; interestingly, **8** and **9** showed better response than **6** and **7**. After 50 s of exposure, the initial fluorescence intensity of **8** decreased about 80%, whereas for **6** it was only 16%.

We observed that the acid analogues **8** and **9** have higher quenching efficiency than the esters **6** and **7**. As evident from the crystal structure, the acid molecules can orient themselves in a regular repetitive 2-D motif (Figure 14).

We propose that through-space long-range exciton migration was possible in **8** and **9** due to the structural pattern and close proximity of the neighboring molecules, which in turn helped signal amplification.[38] As evidenced from the X-ray structure,

DOI: 10.1021/acs.joc.5b00348
J. Org. Chem. 2015, 80, 4064−4075

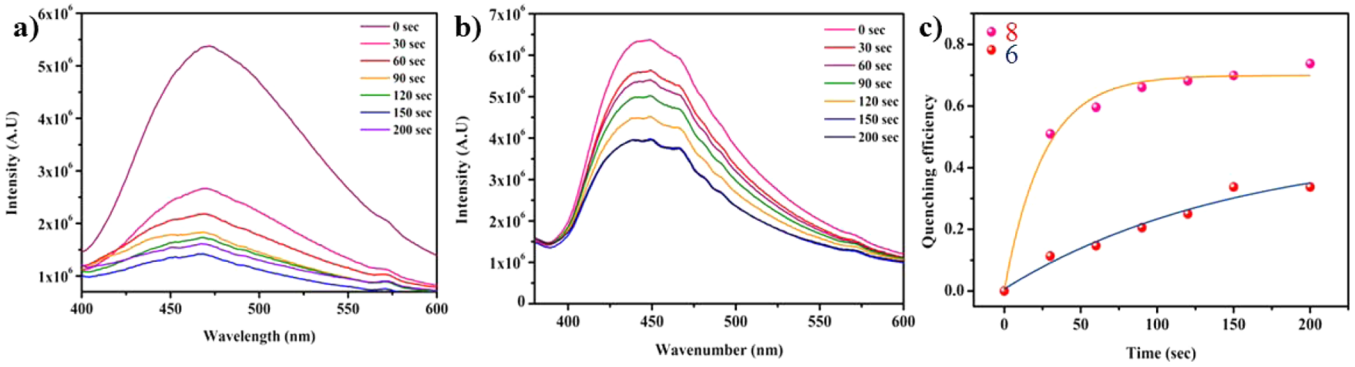

Figure 13. (a) Titration of **8** wth NB, (b) titration of **6** with NB, and (c) quenching efficiency of both the compounds (**6** and **8**).

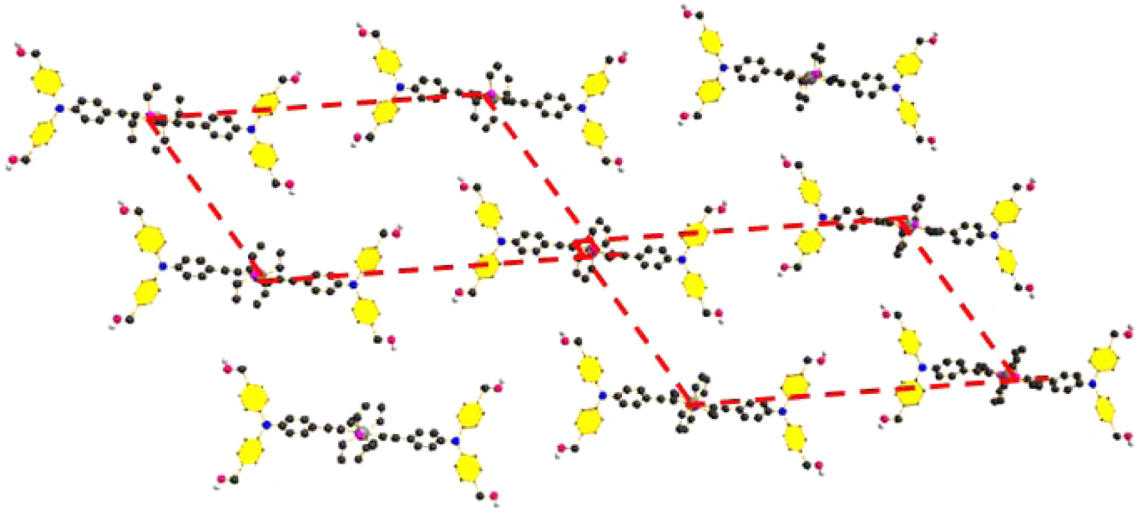

Figure 14. 2D structural pattern of **8** as observed from crystal structure.

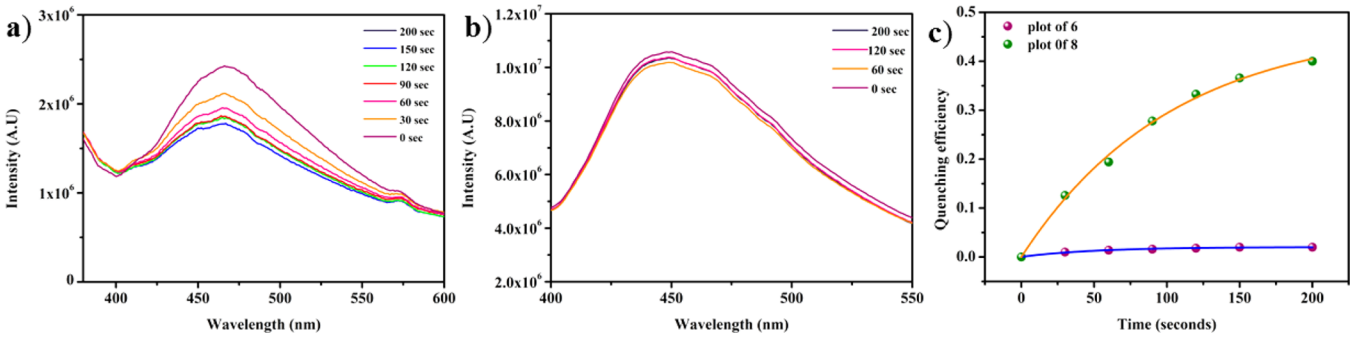

Figure 15. (a) Quenching of fluorescence intensity of the thin films of **8** and (b) **6** upon exposure to PA vapor. (c) Quenching efficiency of **6** and **8** together.

the ester analogues are not arranged in a regular 2-D motif; rather, they are oriented in a zigzag pattern, which is not favorable for long-range exciton migration. Although NB did not show any significant quenching in solution, this anomalous behavior in the solid state can be attributed to relatively high vapor pressure of NB among the tested nitro-aromatic compounds. Although PA has much lower vapor pressure, we have tested the quenching of solid-state fluorescence intensity of the compounds in the presence of PA vapor with time (Figure 15). For **8**, 40% of the initial fluorescence intensity was quenched upon 90 s exposure, but the intensity of **6** was almost unaffected even after exposure to PA for the same amount of time.

To check the reusability of the films, NB was used as analyte, as it showed the maximum quenching efficiency and it could be easily removed by simple heating. Thin films of **9** were first exposed to saturated vapor of NB at room temperature for 100 s, and the change in fluorescence intensity with respect to unexposed film was measured. Gentle heating of the thin film removed the volatile NB and the film was used for fluorescence measurement again and again (Figure 16). However, the quenching efficiency of thin film gradually decreased with the number of cycles.

Theoretical Study. The fluorescence quenching mechanism can be explained by the donor−acceptor electron-transfer mechanism between the sensors and the picrate anion. The

DOI: 10.1021/acs.joc.5b00348
J. Org. Chem. 2015, 80, 4064−4075

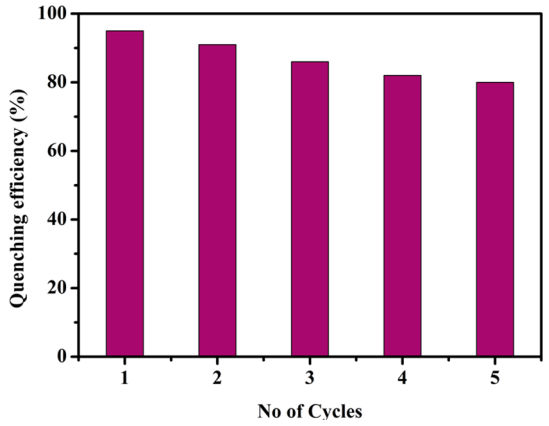

Figure 16. Fluorescence quenching efficiency vs number of cycles for compound **9**.

HOMO−LUMO energy calculation of the sensors along with PA and picrate by gas-phase DFT analysis revealed that the LUMOs of **8** and **9** reside below the HOMO energy level of picrate; thus, electron migration from picrate to the sensors is possible. However, the LUMO of PA is situated above the HOMO energy level of the sensors (HOMO−LUMO gap is higher); therefore, the possibility of ground-state charge transfer from sensor to PA is low. A representative MO diagram of **9** and PA (Figure 17) established that electron transfer from the HOMO of picrate to LUMO of **9** in the ground state is possible leading to static quenching of the fluophore.

Mechanism of Detection. From solution-state fluorescence titration, ^{1}H NMR titration, and theoretical calculations it was found that depending on the solvent used to carry out those experiments the analyte can undergo deprotonation to form picrate anion in the medium. From UV−vis study, the existence of a charge-transfer band was established; in addition, from theoretical calculation the feasibility of ground-state charge-transfer complex formation between **6**, **7**, **8**, **9**, and picrate was elucidated. Thus, in DMA, DMF, and DMSO, PA undergoes deprotonation to form picrate anion, which in turn participated in ground-state charge-transfer complex formation with **8** and **9**. In $CHCl_3$, PA could not undergo deprotonation; therefore, charge transfer between **6**, **7**, and PA in $CHCl_3$ was negligible in solution.[14,37] However, the high quenching by PA may not be only due to ground-state charge migration. When the UV−vis spectra of the analytes were carefully analyzed we observed that absorbance of picrate has strong overlap with emission spectra of the compounds (Figure 18).

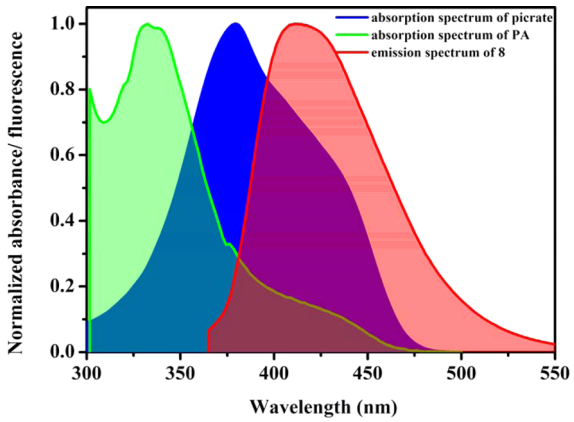

Figure 18. Spectral overlap between absorption spectra of PA and picrate with emission spectra of **8**.

PA has considerably lower spectral overlap than picrate. Resonance energy transfer from fluorophore to picrate could be another pathway of quenching of fluorescence due to considerable spectral overlap of picrate with the analytes (Figure 18 and Supporting Information). Therefore, in solution both charge-transfer and resonance energy transfer contributed to the amplified quenching of fluorescence of the present systems.

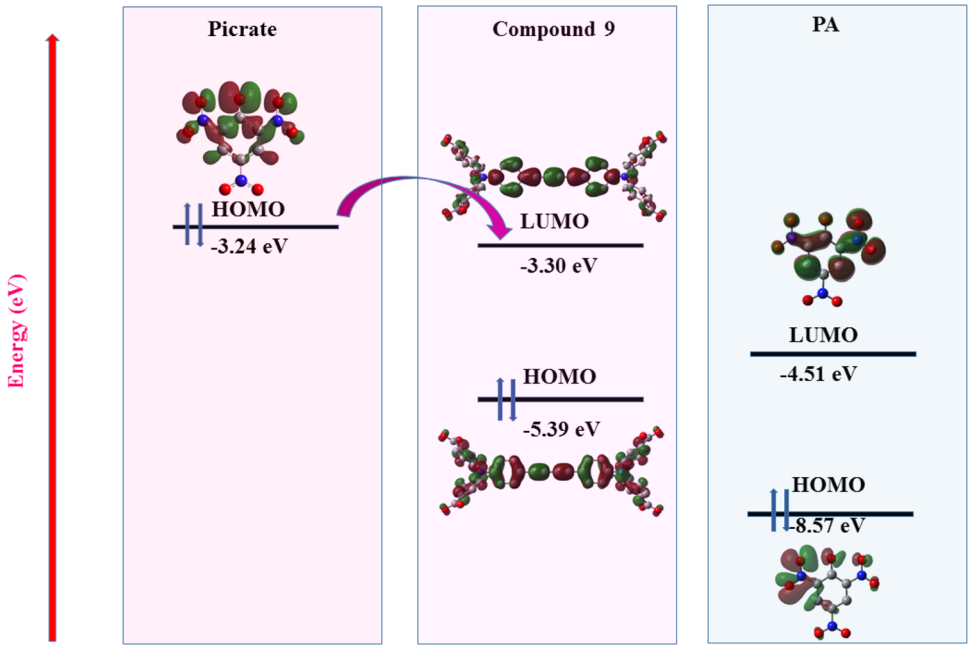

Figure 17. Calculated energy level diagram of **9**, PA, and picrate.

DOI: 10.1021/acs.joc.5b00348
J. Org. Chem. 2015, 80, 4064−4075

However, in the solid state, the molecules **8** and **9** could orient in a 2-D patterned structure as observed from the crystal structure of **8**. Thus, upon analyte binding long-range exciton migration could occur, which led to the amplified sensing of the carboxylic acid sensors, yet the ester molecules **6** and **7** could not organize in such a gridlike pattern. Thus, exciton migration might be disturbed in ester molecules, and they exhibited less quenching.

CONCLUSION

In conclusion, four TPA-based compounds for efficient and fast detection of PA have been developed. The phenyl ring near the ethynyl group formed stable electron donor−acceptor complexes with electron-rich picrate anion. From photophysical studies it was evident that the compounds underwent concentration-dependent aggregation by $\pi-\pi$ interaction. Solution-state fluorescence titration study revealed that all of the compounds have very high binding affinity for picrate and the quenching of fluorescence was due to picrate to sensor charge transfer in ground-state complex formation as well as resonance energy transfer between picrate and the sensors. In the vapor phase, the acids **8** and **9** exhibited higher sensitivity than the esters **6** and **7**, which is presumably due to exciton migration through the neighboring molecules.

EXPERIMENTAL SECTION

Materials and Methods. All chemicals were purchased from commercially available sources and used without further purification. Triethylamine and toluene were distilled over sodium before use. Compound **1** was synthesized by following a previously reported procedure.[39] Compounds **2** and **3** were also synthesized according to the procedure already reported in the literature.[40] The NMR spectra were recorded using a 400 MHz NMR spectrometer. The chemical shifts (δ) in ^{1}H NMR were reported in ppm relative to tetramethylsilane (Me_4Si) as internal standard (0.0 ppm) or proton resonance resulting from incomplete deuteration of NMR solvent: $CDCl_3$ (7.26) and DMSO-d_6 (2.50). ^{13}C NMR spectra were recorded at 100 MHz, and the chemical shifts (δ) are reported ppm relative to external $CDCl_3$ and DMSO-d_6 at 77.8−77.2 and 40.50 ppm, respectively. The ^{31}P NMR spectra were recorded at 120 MHz, and the chemical shifts (δ) are reported in ppm relative to external 83% H_3PO_4 at 0.0 ppm. Electrospray ionization mass spectra were recorded using Esquire 3000 plus ESI and Q-TOF mass spectrometers. Electronic absorption spectra and emission spectra were recorded on a LAMBDA 750 UV/vis spectrophotometer and HORIBA JOBIN YVON made Fluoromax-4 spectrometer. For absorption and emission studies, solutions were prepared using a microbalance and volumetric glassware and charged into quartz cuvettes. Single-crystal X-ray diffraction data were collected with a SMART APEX diffractometer equipped with a three-axis goniometer. The data were integrated by using SAINT, and an empirical absorption correction was applied by SADABS. The structures were determined by direct methods using SHELX-97. Time resolved fluorescence measurements were carried out on an IBH-Data station platform using 425 and 470 nm nano-LED sources.

Synthesis of 4. A flame-dried, 100 mL, two-neck, round-bottom flask was charged with **3** (2.00 g, 4.54 mmol), CuI (0.043 g, 0.22 mmol), PPh_3 (0.117 g, 0.44 mmol), and $Pd(PPh_3)_2Cl_2$ (0.10 g, 0.14 mmol) in freshly distilled triethylamine (40 mL) under nitrogen atmosphere and heated for 15 min at 50 °C. Trimethylsilylacetylene (1.9 mL, 13.64 mmol) was added dropwise to the mixture under high nitrogen flow, and the reaction mixture was refluxed for 36 h. The solvent was removed under vacuum, and the crude was purified by column chromatography using ethyl acetate (EA)/hexane (20%) to afford a yellow solid product (1.60 g) in 77% yield. ^{1}H NMR ($CDCl_3$, 400 MHz): δ 7.92 (d, J = 8 Hz, 4H), 7.41 (d, J = 8 Hz, 2H), 7.08 (d, J = 8 Hz, 4H), 7.04 (d, J = 8 Hz, 2H), 3.81 (s, 6H), 0.24 (s, 9H). ^{13}C NMR (100 MHz, $CDCl_3$): δ = 166.9, 151.1, 146.8, 133.9, 131.6, 125.8, 123.5, 119.7, 104.8, 95.3, 52.5. Anal. Calcd (vacuum-dried sample) for $C_{27}H_{27}NO_4Si$: C, 70.87; H, 5.95; N, 3.06. Found: C, 70.75; H, 5.67; N, 3.29.

Synthesis of 5. A mixture of compound **4** (1.50 g, 3.27 mmol) and K_2CO_3 (1.80 g, 13.02 mmol) was dissolved in a solvent mixture of dichloromethane (DCM) and methanol (MeOH) (20:30) and stirred for 24 h. The solvent was removed under reduced pressure, and the crude was purified by column chromatography using DCM/hexane (1:4) as eluent to obtain an off-white solid (1.14 g) in 90% yield. ^{1}H NMR ($CDCl_3$, 400 MHz): δ 7.93 (d, J = 8 Hz, 4H), 7.43 (d, J = 8 Hz, 2H), 7.08 (d, J = 8 Hz, 4H), 7.04 (d, J = 8 Hz, 2H), 3.89 (s, 6H), 3.08 (s, 1H). ^{13}C NMR (100 MHz, $CDCl_3$): δ = 166.9, 151.0, 147.0, 134.0, 131.6, 125.8, 125.4, 123.6, 118.7, 83.6, 52.4, 31.3. Anal. Calcd (vacuum-dried sample) for $C_{24}H_{19}NO_4$: C, 74.79; H, 4.97; N, 3.63. Found: C, 74.25; H, 4.62; N, 3.59.

Synthesis of 6. To a freshly distilled mixture of toluene (30 mL) and diethylamine (15 mL) in a Schlenk flask were added **5** (1.35 g, 3.50 mmol), *trans*-$Pt(PEt_3)_2I_2$ (1.00 g, 1.46 mmol), and CuI (0.06 g, 0.32), and the flask was degassed under vacuum and refilled with nitrogen for three times. The reaction mixture was stirred for 48 h at room temperature. The solvent was removed under vacuum, and the crude was purified by column chromatography using ethyl acetate/hexane (1:1) as eluent to afford **6** as a yellow solid (1.10 g) in 63% yield with respect to *trans*-$Pt(PEt_3)_2I_2$. ^{1}H NMR ($CDCl_3$, 400 MHz): δ 7.89 (d, J = 12 Hz, 4H), 7.23 (d, J = 8 Hz, 2H), 7.08 (d, J = 8 Hz, 4H), 6.96 (d, J = 12 Hz, 2H), 3.88(s, 12H), 2.19 (m, 12H), 1.23 (m, 18H). ^{13}C NMR (100 MHz, $CDCl_3$): δ = 166.9, 151.4, 143.5, 133.0, 131.2, 127.0, 124.6, 122.9, 84.2, 52.7, 22.9, 16.9, 8.8. ^{31}P NMR (120 MHz, $CDCl_3$) δ = 11.25. IR (cm^{-1}) ν = 2949 (w), 2102 (s), 1716 (s), 1573 (s), 1491 (s), 1429 (m), 1261 (m), 1955 (s), 1086 (w), 1018 (w), 818 (w), 770 (w), 694 (w), 532 (w). HRMS (ESI): $C_{60}H_{66}N_2O_8P_2Pt$ $(M + H)^+$ = 1200.3914 found 1200.3968 (100%). Anal. Calcd (vacuum-dried sample) for $C_{60}H_{66}N_2O_8P_2Pt$: C, 60.04; H, 5.54; N, 2.33. Found: C, 60.35; H, 5.27; N, 2.79. Melting point range (167−176 °C).

Synthesis of 7. Compound **5** (1.40 g, 3.63 mmol) was dissolved in 100 mL of dichloromethane (DCM). To the above solution, CuCl (15.50 g, 156.58 mmol) and tetramethylethylenediamine (TMEDA) (18.14 g, 156.05 mmol) were added, and the mixture was stirred overnight. The organic solvent was concentrated, filtered through Celite, and washed several times. The solvent was removed, and the crude product was purified by column chromatography using DCM/hexane (20%) to obtain **7** as a bright yellow solid (1.3 g) in 93% yield. ^{1}H NMR ($CDCl_3$, 400 MHz): δ 7.94 (d, J = 8 Hz, 8H), 7.45 (d, J = 8 Hz, 4H), 7.11 (d, J = 8 Hz, 8H), 7.06 (d, J = 8 Hz, 4H), 3.90 (s, 12H). ^{13}C NMR (100 MHz, $CDCl_3$): δ = 166.9, 150.9, 147.4, 134.4, 131.6, 125.7, 125.3, 123.9, 117.9, 82.0, 52.5. IR (cm^{-1}) ν = 2949 (w), 1704 (s), 1585 (s), 1504 (s), 1423 (s), 1311 (s), 1261 (m), 1167 (s), 1099 (s), 825 (m), 756 (m), 675 (m). Anal. Calcd (vacuum-dried sample) for $C_{48}H_{36}N_2O_8$: C, 74.99; H, 4.72; N, 3.64. Found: C, 74.75; H, 4.17; N, 3.59. Melting point range (>200 °C).

Synthesis of 8. In a flame-dried, 100 mL, round-bottom flask, **6** (0.12 g, 0.10 mmol) was dissolved in a mixture of 20 mL of MeOH and 30 mL of THF. The mixture was stirred at room temperature for 15 min followed by addition of 20 mL of NaOH solution (0.016 g, 0.4 mmol) in water. The mixture was refluxed for 24 h (monitored by TLC). The volatile solvents were removed using high vacuum, and the residue was acidified with dilute acetic acid to generate yellow precipitate. The precipitate was collected, washed several times with water, and dried under vacuum to afford **8** as a yellow solid (0.09 g) in 78% yield. ^{1}H NMR (DMSO-d_6, 400 MHz): δ 7.82 (d, J = 8 Hz, 8H), 7.17 (d, J = 8 Hz, 4H), 6.99 (m, 12H). ^{13}C NMR (100 MHz, $CDCl_3$): δ =168.4, 150.4, 143.8, 132.8, 131.7, 128.3, 126.9, 123.9, 122.8, 92.0, 84.2, 16.9, 9.3. ^{31}P NMR (120 MHz, $CDCl_3$) δ = 12.13. IR (cm^{-1}) v = 3410 (b), 2949 (b), 2525 (b), 2090 (m), 1672 (s), 1579 (s), 1491 (s), 1367 (m), 1261 (s), 1168 (s), 831 (w), 762 (m), 700 (w), 557 (w). HRMS (ESI): $C_{56}H_{58}N_2O_8P_2Pt$ $(M + H)^+$ = 1144.3331, found 1144.3352 (100). Anal. Calcd (vacuum-dried sample) for

DOI: 10.1021/acs.joc.5b00348
J. Org. Chem. 2015, 80, 4064−4075

$C_{56}H_{58}N_2O_8P_2Pt$: C, 58.79; H, 5.11; N, 2.45. Found: C, 58.25; H, 5.67; N, 2.29. Melting point (>200 °C).

Synthesis of 9. In a flame-dried, 100 mL, round-bottom flask, **7** (0.12 g, 0.15 mmol) was dissolved in a mixture 20 mL of MeOH and 30 mL of THF. The mixture was stirred at room temperature for 15 min followed by addition of 20 mL of NaOH (0.016 g, 0.4 mmol) solution in water.The mixture was refluxed for 24 h (monitored by TLC). The volatile solvent was removed, and the residue was acidified with dilute acetic acid to give a yellow precipitate. The precipitate was collected, washed several times with water, and dried under vacuum to afford **8** as a yellow solid (0.10 g) in 93% yield. ^{1}H NMR (DMSO-d_6, 400 MHz): δ 7.90 (d, J = 8 Hz, 8H), 7.57 (d, J = 8 Hz, 4H), 7.13 (d, J = 8 Hz, 8H), 7.09(d, J = 12 Hz, 4H). ^{13}C NMR (100 MHz, $CDCl_3$): δ = 172.7, 155.5, 153.0, 139.7, 138.2, 136.8, 131.6, 130.4, 129.3, 121.3, 84.6, 79.4. IR (cm^{-1}) v = 2911(b), 2140(w), 1680(s), 1585(s), 1490(s), 1392(m), 1298(m), 1254(s), 1167(s), 1092(m), 756(m), 545(m). HRMS (ESI): $C_{44}H_{28}N_2O_8$ $(M + H)^+$ = 713.1924, found 713.2065 (100). Anal. Calcd (vacuum-dried sample) for $C_{44}H_{28}N_2O_8$: C, 74.15; H, 3.96; N, 3.93. Found: C, 74.05; H, 3.87; N, 3.79. Melting point (>200 °C).

Computational Study. The geometries of the compounds **6**–**9**, PA, and picrate were optimized by the density functional method (DFT) using B3LYP functional, 631-G, and LanL2DZ as the basis sets in the Gaussian (09) program.

Fluorescence Experiments in Solution State. For fluorescence titration, a 2 mL stock solution (1×10^{-7} M) of the corresponding compound was placed in a quartz cell of 1 cm width, and the quencher (1.0×10^{-5} M) solution was gradually added in an incremental fashion. Their corresponding fluorescence emission spectra were recorded at 298 K. For all measurements, compounds **6**–**9** were excited at their respective absorption maxima, and their corresponding emission wavelength was monitored. Both excitation and emission slit widths were 2 nm for all the measurements. The static quenching constants were estimated from steady-state fluorescence quenching. The Stern–Volmer quenching constant was calculated employing the fluorescence emission intensity ratio (I_0/I) as a function of increasing quencher concentration ([Q]) using the equation $I_0/I = 1 + K_{SV}[Q]$. For the selectivity test, a 400 μL (10^{-5} M) solution of each quencher is added at one time into 2 mL of chloroform (for **6** and **7**) or DMA (for **8** and **9**) solution (10^{-7} M) of the sensor. The fluorescence efficiency was plotted as $[(I_0 - I)/I_0]$ vs the quencher concentration, where I_0 and I are the fluorescence intensities before and after addition of quencher. The fluorescence lifetime of the sensors were measured by fitting the fluorescence decay with double exponential convolved with instrumental reference. For the sensitivity measurement, PA solutions of different concentrations were prepared and added gradually to the sensor solution (2×10^{-7} M) in chloroform or DMA. The solvent-dependent fluorescence of the sensors was measured by making a 2 mL 10^{-5} M solution of the sensors in the corresponding solvents from initial stock solution either in chloroform (**6** and **7**) or in DMA (**8** and **9**). For contact-mode detection of PA, a 0.1 mM solution of the corresponding compound was prepared. For the concentrated solution Whatman 42 filter paper strips (4 cm^2 areas) were dipped and dried under vacuum. The dried strips were used for further experiments.

Preparation of Thin Layers and Solid-State Fluorescence Study. To make the thin layers of the sample on the quartz slide, 10 μL saturated solutions of compounds in either $CHCl_3$ or DMA were placed on the cleaned air-dried quartz slide. The slides were kept inside a desiccator and dried under vacuum for 2 h. New slides with a thin layer were used for each of the fluorescence-quenching experiments. The original fluorescence spectra of new films were recorded before and after exposing to the vapor of corresponding quenchers. For liquid analytes, 2 mL of each compound was placed in small (10 mL) glass beakers, a thin layer of cotton is placed above the sample to prohibit direct contact of the analyte with thin film, and the beaker finally was covered by aluminum foil for several days to ensure that the equilibrium vapor pressure of the analytes was achieved. The original fluorescence spectra of the thin layers were recorded before putting the glass slide into the beakers containing the analytes. After the specified exposure time, the slide was taken out and without any further delay mounted to the sample holder of the fluorescence spectrophotometer, and the emission spectra were recorded. For solid samples, 1 g of each quencher was placed in a 10 mL beaker as mentioned for liquid analytes. Solid-state sensing was repeated at least three times to obtain reliable data.

NMR Titration. In the NMR titration experiments, 400 μL of the sample solution was taken in a normal NMR tube, to which PA solution of the same strength was added in incremental fashion, and the changes in chemical shifts of the protons were monitored.

■ ASSOCIATED CONTENT

Supporting Information

^{1}H, ^{13}C, and ^{31}P NMR of the compounds, ESI-MS, UV/vis, fluorescence spectra, NMR titration plots, and table for optimized coordinates. This material is available free of charge via the Internet at http://pubs.acs.org.

■ AUTHOR INFORMATION

Corresponding Author

*E-mail: psm@ipc.iisc.ernet.in.

Notes

The authors declare no competing financial interest.

■ ACKNOWLEDGMENTS

A.C. is thankful to Samya Banerjee for HRMS experiments. We thank Prodip Howlader and Bijan Roy for theoretical calculations. A.C and P.S.M are thankful to CSIR (India) and DST (India) for a research fellowship and financial support (Swarnajayanti Fellowship grant), respectively.

■ REFERENCES

(1) Akhavan, J. *Chemistry of Explosives*, 2nd ed; Royal Society of Chemistry: London, 2004.
(2) Cooper, P. *Explosive Engineering*; Wiley-VCH: New York, 1996; p 33.
(3) Hamrick, J. T. U.S. Patent 3515604, June 2, 1970.
(4) Muthurajan, H.; Shivabalan, R.; Talwar, M. B.; Asthana, S. N. *J. Hazard. Mater.* **2004**, *112*, 17–33.
(5) Beyer, C.; Bohme, U.; Pietzsch, C.; Roewer, G. *J. Organomet. Chem.* **2002**, *654*, 187–201.
(6) Bingham, E., Cohrssen, B.; Powell, C. H. *Patty's Toxicology*; John Wiley & Sons: New York, 2000; Vol. *IIB*, p 980.
(7) Safety data sheet for picric acid, resource of National Institutes of Health.
(8) Ashbrook, P. C.; Houts, T. A. *ACS. Div. Chem. Health Safety* **2003**, *10*, 27–25.
(9) Cameron, M. *Picric Acid Hazards*; American Industrial Hygiene Association: Fairfax, VA, 1995.
(10) Wyman, J. F.; Serve, M. P.; Hobson, D. W.; Lee, L. H.; Uddin, D. E. *J. Toxicol. Environ. Health, Part A* **1992**, *37*, 313–316.
(11) Anderson, G.; Lamer, J. D.; Charles, P. T. *Environ. Sci. Technol.* **2007**, *41*, 2888–2893.
(12) Sylvia, J. M.; Janni, J. A.; Klein, J. D.; Spencer, K. M. *Anal. Chem.* **2000**, *72*, 5834–5840.
(13) (a) Krausa, M.; Schorb, K. J. *Electroanal. Chem.* **1999**, *461*, 10–13. (b) Hakansson, K.; Coorey, R. V.; Zubarev, R.; Talrose, V. L.; Hakansson, P. *J. Mass Spectrom.* **2000**, *35*, 337–346.
(14) (a) Roy, B.; Bar, A. K.; Gole, B.; Mukherjee, P. S. *J. Org. Chem.* **2013**, *78*, 1306–1310. (b) Samanta, D.; Mukherjee, P. S. *Dalton. Trans.* **2013**, *42*, 16784–16795. (c) Vajpayee, V.; Kim, H.; Mishra, A.; Mukherjee, P. S.; Stang, P. J.; Lee, M.; Kim, H. K.; Chi, K. W. *Dalton Trans.* **2011**, *40*, 3112–3115. (d) Ghosh, S.; Mukherjee, P. S. *Organometallics* **2008**, *27*, 316–319. (e) Shanmugaraju, S.; Jadav, H.; Patil, P. Y.; Mukherjee, P. S. *Inorg. Chem.* **2012**, *51*, 13072–13074. (f) Shanmugaraju, S.; Joshi, S. A.; Mukherjee, P. S. *Inorg. Chem.* **2011**, *50*, 11736–11745.

DOI: 10.1021/acs.joc.5b00348
J. Org. Chem. 2015, 80, 4064–4075

(15) (a) Jiang, Y.; Zhao, H.; Zhu, N.; Lin, Y.; Yu, P.; Mao, L. *Angew. Chem., Int. Ed.* **2008**, *47*, 8601−8604. (b) Ma, Y.; Li, H.; Peng, S.; Wang, L. *Anal. Chem.* **2012**, *84*, 8415−8421. (c) Dasary, S. S. R.; Singh, A. K.; Senapati, D.; Yu, H.; Ray, P. C. *J. Am. Chem. Soc.* **2009**, *131*, 13806−13812. (d) Feng, L.; Li, H.; Qu, Y.; Lu, C. *Chem. Commun.* **2012**, *48*, 4633−4635.
(16) (a) Yag, Y.; Wang, H.; Su, K.; Long, Y.; Peng, Z.; Li, N.; Feng, L. *J. Mater. Chem.* **2011**, *21*, 11895−11900. (b) Liao, Y. Z.; Strong, V.; Wang, Y.; Li, X.; Wang, X.; Kaner, R. B. *Adv. Funct. Mater.* **2012**, *22*, 726−735.
(17) (a) Thomas, S. W., III; Joly, G. D.; Swager, T. M. *Chem. Rev.* **2007**, *107*, 1339−1386. (b) Kim, D. S.; Lynch, V. M.; Nielsen, K. A.; Johnsen, C.; Jeppesen, J. O.; Sessler, J. L. *Anal. Bioanal. Chem.* **2009**, *395*, 393−400. (c) He, G.; Peng, H.; Liu, T.; Yang, M.; Zhang, Y.; Fang, Y. *J. Mater. Chem.* **2009**, *19*, 7347−7353. (d) Hu, Y. J.; Tan, S. Z.; Shen, G. L.; Yu, R. Q. *Anal. Chim. Acta* **2006**, *570*, 170−175. (e) Nie, H.; Zhao, Y.; Zhang, M.; Ma, Y.; Baumgarten, M.; Mullen, K. *Chem. Commun.* **2011**, *47*, 1234−1236. (f) Nagarkar, S. S.; Joarder, B.; Chaudhari, A. K.; Mukherjee, S.; Ghosh, S. K. *Angew. Chem., Int. Ed.* **2013**, *52*, 2881−2885.
(18) (a) Bhalla, V.; Gupta, A.; Kumar, M.; Rao, D. S. S.; Prasad, S. K. *ACS. Appl. Mater. Interfaces.* **2013**, *5*, 672−679. (b) Dey, N.; Samanta, S. K.; Bhattacharya, S. B. *ACS. Appl. Mater. Interfaces.* **2013**, *5*, 8394−8400.
(19) (a) Gole, B.; Bar, A. K.; Mukherjee. *Chem.—Eur. J.* **2014**, *20*, 2776−2783. (b) Xu, H.; Liu, F.; Cui, Y.; Chen, B.; Qian, G. *Chem. Commun.* **2011**, *47*, 3153−3155. (c) Gole, B.; Bar, A. K.; Mukherjee, P. S. *Chem. Commun.* **2011**, *47*, 12137−12139.
(20) Ni, R.; Tong, R. B.; Guo, C. C.; Shen, G. L.; Yu, R. Q. *Talanta* **2004**, *63*, 251−257.
(21) Bhalla, V.; Gupta, A.; Kumar, M. *Org. Lett.* **2012**, *14*, 3112−3115.
(22) Yongqian, X.; Benhao, L.; Weiwei, L.; Jie, Z.; Shiguo, Sun.; Yi, P. *Chem. Commun.* **2013**, *49*, 4764−4766.
(23) (a) Yang, J.-S.; Swager, T. M. *J. Am. Chem. Soc.* **1998**, *120*, 5321−5322. (b) Yang, J. S.; Swager, T. M. *J. Am. Chem. Soc.* **1998**, *120*, 11864−11873.
(24) (a) Bernstein, J.; Davis, R. E.; Shimoni, L.; Chang, N. L. *Angew. Chem., Int. Ed.* **1995**, *107*, 1689−1708. (b) Etter, M. C. *Acc. Chem. Res.* **1990**, *23*, 120−126.
(25) (a) Gole, B.; Shanmugaraju, S.; Bar, A. K.; Mukherjee, P. S. *Chem. Commun.* **2011**, *47*, 10046−10048. (b) Gole, B.; Song, W.; Lackinger, M.; Mukherjee, P. S. *Chem.—Eur. J.* **2014**, *20*, 13662−13680.
(26) (a) Meier, B. H.; Graf, F.; Ernst, R. R. *J. Chem. Phys.* **1992**, *76*, 767−769. (b) Lifson, S.; Hagler, A. T.; Dauber, P. *J. Am. Chem. Soc.* **1979**, *101*, 5111−5121.
(27) Liu, Y.; Chen, X.; Lv, Y.; Chen, S.; Lam, J. W. Y.; Mahtab, F.; Kwok, H. S.; Tao, S.; Tang, B. Z. *Chem.—Eur. J.* **2012**, *18*, 9929−9938.
(28) (a) Gao, Y.; Qu, Y.; Jiang, T.; Zhang, H.; Nannan, H.; Bo, L.; unchen, W.; Hua, J. *J. Mater. Chem. C* **2014**, *2*, 6353−6361. (b) Qu, Y.; Zhang, X.; Yonqquan, W.; Fuyou, L.; Hua, L. *Polymer Chem.* **2014**, *5*, 3396−3403.
(29) (a) Ning, Z.; Chen, Z.; Zhang, Q.; Yan, Y.; Qian, S.; Cao, Y.; Tian, H. *Adv. Funct. Mater.* **2007**, *17*, 3799−3807. (b) Li, H.; Chi, Z.; Xu, B.; Zhang, X.; L, X.; Liu, S.; Zhang, Y.; Jiarui, X. *J. Mater. Chem.* **2011**, *21*, 3760−3767. (c) Yuan, W. Z.; Lu, P.; Chen, S.; Lam, J. W. Y.; Wang, Z.; Liu, Y.; Kwok, H. S.; Ma, Y.; Tang, B. Z. *Adv. Mater.* **2010**, *22*, 2159−2163. (d) Wang, J.; Mei, J.; Hu, R.; Sun, Z. J.; Qin, A.; Tang, B. Z. *J. Am. Chem. Soc.* **2012**, *134*, 9956−9966.
(30) (a) Pati, P. B.; Zade, S. S. *Tetrahedron Lett.* **2014**, *55*, 5290−5293. (b) Wenfeng, L.; Hengchang, M.; Ziqiang, L. *RSC. Adv.* **2014**, *4*, 39351−39358. (c) Zhao, Z.; Liu, Z.; Lam, J. W. Y.; Chan, C. Y. K.; Qiu, H.; Tang, B. Z. *Dyes Pigments* **2011**, *91*, 258−263.
(31) (a) Rosch, U.; Yao, S.; Wortmann, R.; Wurthner, F. *Angew. Chem., Int. Ed.* **2006**, *45*, 7026−7030. (b) Wurth, C.; Grabolle, M.; Pauli, J.; Spieles, M.; Resch-Genger, U. *Nat. Protocols* **2013**, *8*, 1535−1550.
(32) Hamerer, F.; Garcia, G.; Chen, S.; Florent, P.; Achelle, S.; Fiorni, C.; Mailard, P. *J. Org. Chem.* **2014**, *79*, 1406−1417.
(33) (a) Banal, J. A.; White, J. M.; Ghiggino, K. P.; Wong, W. H. *Nat. Sci. Rep.* **2014**, *4*, 4635−4640. (b) Shetty, A. S.; Zhang, J.; Moore, J. S. *J. Am. Chem. Soc.* **1996**, *118*, 1019−1027. (c) Wurthner, F.; Chen, Z.; Dehm, V.; Stepanenko, V. *Chem. Commun.* **2006**, 1188−1190. (d) Yoneda, k.; Nakano, M.; Fukuda, K.; Matsui, H.; Takamuku, S.; Hirosaki, Y.; Kubo, T.; Kamada, K.; Champagne, B. *Chem.—Eur. J.* **2014**, *20*, 11192. (e) Markova, L. I.; Malinovski, V.; Patsenker, L. D.; Haner, R. *Chem. Commun.* **2013**, *49*, 5298−5300.
(34) (a) Ding, L.; Bai, Y.; Cao, Y.; Ren, G.; Blanchard, G. J.; Fang, Y. *Langmuir* **2014**, *30*, 7645−7653. (b) Venkatramaiah, N.; Kumar, S.; Patil, S. *Chem.—Eur. J.* **2012**, *18*, 14745−14751. (c) Kumar, S.; Venkatramaiah, N.; Patil, S. *J. Phys. Chem. C* **2013**, *117*, 7236−7245. (d) Vajpaye, V.; Kim, H.; Mishra, A.; Mukherjee, P. S.; Stang, P. J.; Lee, M. H.; Kim, H. K.; Chi, K. W. *Dalton. Trans.* **2011**, *40*, 3122−3124. (e) Yang, X.; Niu, C. G.; Shen, G. L.; Yu, R. Q. *Analyst* **2001**, *126*, 349. (f) Xu, B.; Wu, X.; Li, H.; Tong, H.; Wang, L. *Macromolecules* **2011**, *44*, 5089−5092.
(35) (a) Bhalla, V.; Arora, H.; Singh, H.; Kumar, M. *Dalton. Trans.* **2013**, *42*, 969−974. (b) Pramanik, S.; Bhalla, V.; Kumar, M. *Anal. Chim. Acta* **2013**, *793*, 99−106.
(36) (a) Kumar, M.; Reja, S. I.; Bhalla, V. *Org. Lett.* **2012**, *14*, 6084−6087. (b) Zhou, X. H.; Li, L.; Li, H. H.; Li, A.; Yang, T.; Huang, W. *Dalton. Trans.* **2013**, *42*, 12403−12409.
(37) Acharyya, K.; Mukherjee, P. S. *Chem. Commun.* **2014**, *50*, 15788−15791.
(38) (a) Yang, J. S.; Swager, T. M. *J. Am. Chem. Soc.* **1998**, *120*, 11864−11873. (b) McQuade, D. T.; Pullen, A. E.; Swager, T. M. *Chem. Rev.* **2000**, *100*, 2537−2574. (c) Zhou, Q.; Swager, T. M. *J. Am. Chem. Soc.* **1995**, *117*, 12593−12602.
(39) Hammerer, F.; Garcia, G.; Chen, S.; Poyer, F.; Achelle, S.; Debuisschert, C. F.; Fichou, M. P.; Mailard, P. *J. Org. Chem.* **2014**, *79*, 1406−1417.
(40) Wood, C. J.; Robson, K. C. D.; Elliot, P. I. P.; Berlinguette, C. P.; Gibson, E. A. R. *RSC Adv.* **2014**, *4*, 5782−5791.

DOI: 10.1021/acs.joc.5b00348
J. Org. Chem. 2015, 80, 4064−4075